Carbohydrate Polymers 331 (2024) 121861

Contents lists available at ScienceDirect

Carbohydrate Polymers

journal homepage: www.elsevier.com/locate/carbpol

The action of *endo*-xylanase and *endo*-glucanase on cereal cell wall polysaccharides and its implications for starch digestion kinetics in an *in vitro* poultry model

Dimitrios Kouzounis [a], Khoa A. Nguyen [a], Cynthia E. Klostermann [a,b], Natalia Soares [c], Mirjam A. Kabel [a], Henk A. Schols [a,*]

[a] *Laboratory of Food Chemistry, Wageningen University & Research, Bornse Weilanden 9, 6708 WG Wageningen, the Netherlands*
[b] *Biobased Chemistry and Technology, Wageningen University & Research, Bornse Weilanden 9, 6708 WG Wageningen, the Netherlands*
[c] *Huvepharma NV, 2600 Berchem, Belgium*

ARTICLE INFO

Keywords:
In vitro digestion
Prebiotic oligosaccharides
Feed enzymes
Starch digestion kinetics
Endo-xylanase
Endo-glucanase

ABSTRACT

Endo-xylanase and *endo*-glucanase are supplemented to poultry diets in order to improve nutrient digestion and non-starch polysaccharide (NSP) fermentation. Here, the action of these enzymes on alcohol insoluble solids (AIS) from wheat and maize grains as well as its implications for starch digestion in milled grains were evaluated *in vitro*, under conditions mimicking the poultry digestive tract. For wheat AIS, GH11 *endo*-xylanase depolymerized soluble arabinoxylan (AX) during the gizzard phase, and proceeded to release insoluble AX under small intestine conditions. At the end of the *in vitro* digestion (480 min), the *endo*-xylanase, combined with a GH7 *endo*-β-1,4-glucanase, released 30.5 % of total AX and 18.1 % of total glucan in the form of arabinoxylo- and gluco-oligosaccharides, as detected by HPAEC-PAD and MALDI-TOF-MS. For maize AIS, the combined enzyme action released 2.2 % and 7.0 % of total AX and glucan, respectively. Analogous *in vitro* digestion experiments of whole grains demonstrated that the enzymatic release of oligomers coincided with altered grain microstructure, as examined by SEM. In the present study, cell wall hydrolysis did not affect *in vitro* starch digestion kinetics for cereal grains. This study contributes to understanding the action of feed enzymes on cereal NSP under conditions mimicking the poultry digestive tract.

1. Introduction

Cereal grains are a main ingredient in animal feed because of their high starch content (47–69 %, dry matter basis) (Bach Knudsen, 1997). Cereal grains also account for 25–40 % of the crude protein in broiler diets (Elkin, 2002). Next to macro- and micro-nutrients, cereal grains, such as wheat and maize, contain non-starch cell wall polysaccharides (NSP; 10–23 %, dry matter basis), such as arabinoxylan (AX), cellulose and mixed-linked β-glucan (MLG) (Bach Knudsen, 1997, 2014).

The contribution of animal farming to climate change, alongside the food-feed-fuel competition and current geopolitical tensions, have increased the need to optimize the nutritional value of animal feed (Muscat et al., 2020). Although >80 % of starch can be digested in the small intestine of broilers, its complete utilization can be hampered by NSP (Choct & Annison, 1992; Zaefarian et al., 2015). For example, soluble AX has been shown to increase intestinal viscosity, thereby limiting nutrient digestibility (Choct & Annison, 1992). Moreover, the insoluble cell wall matrix has been considered as a physical barrier that encapsulates nutrients (*e.g.* starch, proteins) and hinders their digestibility (Bedford, 2018; Grundy et al., 2022). Still, NSP may positively impact broiler health. In particular, soluble NSP can be fermented by bacteria in the broiler ceca to produce health-promoting bacterial metabolites (*e.g.* short chain fatty acids; SCFAs) (Flint et al., 2012; Pan & Yu, 2013; Svihus et al., 2013). Alongside NSP, undigested (resistant) starch can also be fermented in the hindgut (Regassa & Nyachoti, 2018). Nevertheless, starch fermentation cannot compensate for the loss of metabolizable energy (~30 % loss) following incomplete digestion in the small intestine (Gerrits et al., 2012). Overall, the presence of NSP in diets is important for the digestive health, but can also result in sub-optimal feed utilization and impaired broiler growth.

Current research is focused on better utilizing cereal NSP, in order to enhance the nutritional value of poultry diets. Feed supplementation

* Corresponding author.
E-mail address: henk.schols@wur.nl (H.A. Schols).

https://doi.org/10.1016/j.carbpol.2024.121861
Received 20 October 2023; Received in revised form 21 December 2023; Accepted 22 January 2024
Available online 27 January 2024

with NSP-degrading enzymes (NSPases), predominantly *endo*-xylanase, is a successful strategy for offsetting the negative impact of NSP on animal performance. For example, polymeric AX degradation by supplemented *endo*-xylanase has been linked to decreased intestinal viscosity and pronounced nutrient digestibility (Choct & Annison, 1992; Matthiesen et al., 2021). It is indicative that for wheat-based diets, *endo*-xylanase and *endo*-glucanase supplementation was accompanied by increased ileal digestibility (starch; 3–11 % increase, protein; 5–7 % increase) and by improved productive performance of broilers (Kouzounis et al., 2021; Matthiesen et al., 2021; Meng et al., 2005). Moreover, the *in vivo* formation of arabinoxylo-oligosaccharides (AXOS) by dietary *endo*-xylanase has been shown to improve NSP fermentability to SCFAs and to promote the growth of beneficial gut microbiota in the ceca (Kouzounis et al., 2022; Morgan et al., 2019; Wang et al., 2021).

Endo-β-1,4-xylanase (EC 3.2.1.8) cleaves the β-(1 ➔ 4) bond between two xylosyl units within the AX backbone, generating AXOS. Nevertheless, the presence of arabinosyl residues as well as feruloyl-, *O*-methyl-glucuronoyl- or acetyl- substituents may hinder *endo*-xylanases (Dodd & Cann, 2009; Paës et al., 2012). Therefore, the combined action of *endo*-xylanases and other debranching enzymes can facilitate AX depolymerization, as previously reviewed (Dodd & Cann, 2009). Additionally, due to the close association of AX with cellulose in the cell wall matrix, the combined action of xylanolytic and cellulolytic enzymes is often required for the degradation of plant biomass (Song et al., 2016). For instance, the combination of an *endo*-xylanase with an *endo*-β-1,4-glucanase (EC 3.2.1.4) that hydrolyzes the β-(1 ➔ 4) bond between glucosyl units of the β-glucan backbone, was shown to improve the *in vitro* nutrient release from wheat grains (Meng et al., 2005; Tervilä-Wilo et al., 1996). It has, therefore, been postulated that beyond releasing oligosaccharides, NSPases can improve nutrient digestibility by offsetting the encapsulating effect of insoluble NSP. This hypothesis has been mainly demonstrated *in vitro* by an increased glucose (mainly deriving from starch) and protein release from wheat grains upon *endo*-xylanase supplementation without (Lafond et al., 2015) or with the addition of *endo*-glucanase (Meng et al., 2005; Tervilä-Wilo et al., 1996). Nevertheless, it is doubtful whether the improved feed digestibility observed *in vivo* could be attributed mainly to nutrient de-encapsulation or other aforementioned mechanisms of NSPase action (*e.g.* viscosity reduction, improved intestinal health) (Bedford, 2018; Khadem et al., 2016). Additionally, 10–50 times higher enzyme doses have been used in *in vitro* studies compared to *in vivo* studies (Bedford, 2018; Tervilä-Wilo et al., 1996). In spite of possible limitations, *in vitro* digestion models are important for monitoring the function of new feed additives while reducing animal testing and associated costs (Mota de Carvalho et al., 2021). Consequently, a more detailed *in vitro* study of the action of dietary enzymes towards NSP and its implications for nutrient digestion kinetics is necessary.

The aim of this study is to monitor cereal cell wall degradation by *endo*-xylanase and *endo*-glucanase, under *in vitro* conditions mimicking the poultry digestive tract. The impact of enzyme action on oligosaccharide release, cell wall microstructure and starch digestion kinetics shall be examined *in vitro*. We hypothesize that such *in vitro* approach can reveal novel insights into the mechanism of action of NSP-active enzymes and their use as feed supplements.

2. Materials and methods

2.1. Materials

Whole wheat (*Triticum aestivum*) and maize (*Zea mais*) grains were obtained from Research Diet Services B.V. (Wijk bij Duurstede, The Netherlands). Commercially available feed enzyme preparation (Hostazym X; HX) primarily containing *endo*-β-1,4-xylanase from *Trichoderma citrinoviride* belonging to the glycosyl hydrolase CAZy family 11 (GH11) was provided by Huvepharma NV (Berchem, Belgium). GH7 *endo*-β-1,4-glucanase (E-CELTR; Cel7B; coded here EG7) from *T. longibrachiatum* was obtained from Megazyme (Bray, Ireland). Enzyme activity, as provided by the manufacturers, is mentioned in Table S1. The performance of both enzyme preparations on arabinoxylan and mixed linked β-glucan (MLG) was determined (see supplement 1.3; Table S1). Pepsin from porcine gastric mucosa (610 U/mg) and pancreatin from porcine pancreas (8 × USP) were obtained from Sigma-Aldrich (St Louis, MO, USA). Individual xylo-oligosaccharides (degree of polymerization (DP) 2–6) and cellobiose standards were purchased from Megazyme, whereas glucose, xylose, arabinose, rhamnose, galactose, mannose and galacturonic acid standards were purchased from Sigma-Aldrich. All reagents used were of analytical grade. The water used was from a Milli-Q Integral 5 (Millipore Corp., Billerica, MN, USA) purification system. Specific reagents and enzymes are listed in the respective sections.

2.2. Cereal cell wall material isolation as alcohol insoluble solids (AIS)

The isolation of cell wall material from wheat and maize whole grains as alcohol insoluble solids (AIS) was performed according to Kabel et al. (2002), with several modifications. Whole wheat and maize grains were milled with a 0.5 mm screen to pass a 0.7 mm sieve using a ZM200 mill (Retsch GmbH, Haan, Germany). A schematic overview of AIS isolation is presented in Fig. S1. First, 300 g milled grains were suspended in 1500 mL 200 mM sodium acetate (NaOAc) buffer, pH 5.2. Next, thermostable α-amylase from *Bacillus sp.* (Megazyme) was added (2.25 mL; 3000 U/mL) and the mixture was incubated at 80 °C for 30 min, under continuous stirring. The mixture was then cooled to 40 °C and the same α-amylase (2.25 mL) and amyloglucosidase from *Aspergillus niger* (Megazyme) (3.75 mL; 3260 U/mL) were added. Subsequently, the mixture was incubated for 3 h. Afterwards, the mixture was divided in centrifugal tubes and was centrifuged (15 min, 12,000 ×*g*, 20 °C). The obtained supernatants were collected together and stored at 4 °C. The pellets were combined, resuspended in 750 mL NaOAc buffer, mixed with 2.25 mL α-amylase and 3.75 mL amyloglucosidase and were incubated overnight at 30 °C. The mixture was centrifuged as described above. The supernatants were combined and stored with the previously obtained ones. The pellets were combined, resuspended in 1000 mL NaOAc buffer, mixed with 3.75 mL amyloglucosidase and were incubated at 40 °C for 1 h. Afterwards, all supernatant and pellets were mixed together and the pH value of the suspension was adjusted to pH 6.0. Protease from *B. licheniformis* (Megazyme) (3.75 mL; 300 U/mL) and Flavourzyme (peptidase mixture from *A. oryzae*; Sigma-Aldrich) (1.25 mL; 600–700 U/mL) were added and the mixture was incubated at 50 °C for 1 h. Upon cooling, ethanol was added up to 70 % (v/v) of the total final volume and the mixture was stored overnight at 4 °C. The residue was separated by filtration and collected. The obtained residue was washed four times with 70 % (v/v) ethanol and six times with 96 % (v/v) ethanol, in order to remove all alcohol soluble material. Each washing step involved mixing the residue with the solvent, followed by centrifugation (15 min, 12,000 ×*g*, 20 °C) and removal of the supernatant by filtration. The final obtained residue (AIS) was dried at ambient temperature and homogenized using a ZM200 mill (Retsch GmbH).

2.3. In vitro digestion

2.3.1. In vitro AIS digestion

The ability of HX and EG7 to degrade and solubilize cereal NSP *in vitro*, under conditions mimicking the poultry digestive tract, was determined. The digestive conditions applied in this experiment are based on the *in vitro* digestion model described by Martens, Gerrits, Bruininx and Schols (2018), with several modifications. Digestion experiments were performed in triplicate. HX and EG7 stock solutions were prepared in such a manner to achieve a final enzyme (protein): substrate (AIS) ratio 1:80,000 for HX and EG7, individually. For that, the protein content of both enzyme preparations was determined (Supplement 1.2; Table S1). Approximately 100 mg AIS was weighed in 15 mL

reaction tubes, followed by the addition of 0.5 mL 6 mg/mL ribose (Rib; Carbosynth Ltd., Compton, U.K.) and 1 mL water (AIS treatment without enzyme addition; Untr) or 0.5 mL water and 0.5 mL stock enzyme solution (AIS treatment with HX or EG7) or 0.5 mL water and 0.25 mL HX and 0.25 mL EG7 stock solutions (AIS treatment with HX and EG7; HX + EG7). The mixtures were agitated shortly. Next, 0.8 mL 50 % benzoic acid and 4.2 mL 25 mM HCl were added to achieve a pH 3.2 value in order to prevent microbial growth and to simulate the acidic environment of the gizzard (Svihus, 2011), respectively. The tubes were incubated at 40 °C under head-over-tail agitation. The gizzard phase (Gi) lasted for 60 min. Immediately after sampling (0.3 mL), 3.5 mL 0.5 M potassium phosphate buffer (pH 6.5) was added to simulate small intestine conditions. Incubation under the small intestine phase (SI) proceeded for 480 min. Aliquots (0.3 mL) were collected during Gi at 30, 60 min and during SI at 90, 120, 240 and 480 min (total digestion time), transferred in tubes containing 0.3 mL water (99 °C), and were heated at 99 °C, 15 min. All aliquots were centrifuged (10 min, 15,000 ×*g*, 20 °C) and stored at −20 °C. The obtained supernatants were analyzed for sugar composition after acid hydrolysis (HPAEC-PAD; see Section 2.4), molecular weight distribution (HPSEC-RI; see Section 2.6) and oligosaccharide profile (HPAEC-PAD, MALDI-TOF-MS; see Sections 2.7 & 2.8). Pepsin and pancreatin were omitted from AIS digestions due to their interference with subsequent analyses, after having determined that they did not influence the action of HX and EG7 (see supplement 1.4; Fig. S2).

2.3.2. *In vitro whole grain digestion*

The impact of NSP-degrading enzymes on *in vitro* starch digestion kinetics was monitored using the digestion model described by Martens et al. (2018),with several modifications. Firstly, whole grains were milled with a 0.5 mm screen to pass a 0.7 mm sieve using a ZM200 (Retsch GmbH). Digestion experiments were performed in triplicate. HX and EG7 stock solutions were prepared in such a manner to achieve a final Enzyme (protein):substrate (AIS) ratio 1:40,000 for HX and EG7 individually, based on the AIS content of wheat grains. Approximately 1000 mg milled whole grains was weighed in 50 mL tubes, followed by the addition of 1 mL 180 mg/mL ribose solution, 3.5 mL water (treatment without enzyme addition; Untr) or 3 mL water and 0.25 mL HX and 0.25 mL EG7 stock solutions for whole grains treated with HX and EG7 (treatment with HX and EG7; HX + EG7). The mixtures were agitated shortly. Gastric digestion was initiated by the addition of 2.5 mL 50 % benzoic acid and 12.5 mL porcine pepsin (2.2 mg/mL) in 25 mM HCl, followed by incubation at 40 °C for 60 min, under head-over-tail agitation. 0.15 mL was removed at 60 min, transferred in tubes containing 1.35 mL water and stored in ice bath. Immediately after sampling, 5 mL 0.5 M potassium phosphate buffer (pH 6.5) and 5 mL pancreatin solution (7.5 mg/mL) in 0.5 M potassium phosphate buffer (pH 6.5) were added to the 50 mL tubes to simulate the small intestine conditions, and the incubation proceeded for 480 min. 0.15 mL aliquots were removed at 15, 30, 45, 60, 90, 120, 240, 360 and 480 min, transferred in tubes containing 1.35 mL water and stored in ice bath. Immediately afterwards, the sampled aliquots were centrifuged (10 min, 15,000 ×*g*, 4 °C) and 0.2 mL supernatant was transferred in new reaction tubes containing 0.78 mL water, heated at 99 °C for 15 min, and stored at −20 °C. Amyloglucosidase from *A. niger* (20 μL, 6 AU/mL; Sigma-Aldrich) was added to convert soluble starch degradation products formed by α-amylase present in pancreatin to glucose (Glc). The enzymatic incubation was carried out at pH 6.5, 50 °C for 30 min, followed by inactivation at 99 °C for 15 min. The obtained supernatants were analyzed for released Glc (HPAEC-PAD; see Section 2.5). At the end of *in vitro* digestion, the 50 mL tubes were placed in an ice bath. After 10 min, 2 mL suspension containing sedimented material was removed for SEM imaging (see Section 2.9).

2.4. *Neutral sugar composition analysis by HPAEC-PAD*

The neutral sugar composition of solutes released during AIS digestion (see Section 2.3.1) was determined by high performance anion exchange chromatography with pulsed amperometric detection (HPAEC-PAD), after acid hydrolysis of carbohydrates present with 2 M trifluoroacetic acid (TFA) (Gruppen et al., 1992). Analysis was performed using an ICS7000 HPLC system (Dionex, Sunnyvale, CA) with and ICS7000 ED PAD detector (Dionex), and equipped with a CarboPac™ PA1 IC column (250 mm × 2 mm i.d.) and a CarboPac™ PA guard column (50 mm × 2 mm i.d.). The column temperature was set at 20 °C and the injection volume was 10 μL. Three mobile phases were used: A) 0.1 M NaOH, B) 1 M NaOAc in 0.1 M NaOH and C) Water. Neutral monosaccharides were eluted at 0.4 mL/min with 100 % C (isocratic) for 0–35 min, with post column addition of 0.5 M NaOH (0.1 mL/min) to enable PAD detection. The subsequent elution profile was: 35.1–50 min linear gradient 0–40 % B (100–60 % A); 50.1–55 min isocratic 100 % B, 55.1–63 min isocratic 100 % A; 63.1–78 min isocratic 100 % C with post column addition. Constituent monosaccharide quantification was performed using ribose (Rib) as an internal standard. The relative response factors of Ara, Xyl, Glc, Gal, Man and Rha to Rib were determined in the range of 1–50 (μg/mL). Additionally, Rib concentration in the supernatants was used to calculate the actual volume sampled, thus allowing the estimation of the total volume remaining in the reaction tube during *in vitro* digestion.

2.5. *Starch hydrolysis quantification by HPAEC-PAD*

The amount of Glc corresponding to the starch fraction released during whole grain digestion (see Section 2.3.2) was determined by HPAEC-PAD, using the same instrumentation as in 2.4. Three mobile phases were used: A) 0.1 M NaOH, B) 1 M NaOAc in 0.1 M NaOH and C) Water. Glc and Rib were eluted at 0.3 mL/min with 25 % A/85 % C (isocratic) for 0–25 min. The elution program proceeded with 100 % B (isocratic) from 25.1 to 32 min and 25 % A/85 % C (isocratic) from 32.1 to 38 min. The relative response factor of Glc to Rib, the latter used as internal standard, was determined in the range of 1–50 (μg/mL). Additionally, Rib concentration in the supernatants was determined to calculate the actual volume sampled, thus allowing the estimation of the total volume remaining in the reaction tube during *in vitro* digestion.

2.6. *Molecular weight distribution analysis by HPSEC-RI*

The molecular weight distribution of supernatants at the end of *in vitro* AIS digestion (480 min; see Section 2.3.1) was determined by high performance size-exclusion chromatography with refractive index detection (HPSEC-RI), as previously described (Kouzounis et al., 2022). Analysis was performed using an Ultimate 3000 HPLC System (Dionex Corp., Sunnyvale, CA, USA) equipped with a set of three TSK-Gel Super columns 4000AW, 3000AW, and 2500AW (6 mm ID ×150 mm per column, 6 μm), and a TSK Super AW-L guard column (4.6 mm ID ×35 mm, 7 μm) (Tosoh Bioscience Tokyo, Japan). The HPLC system was coupled to a Shodex RI-101 refractive index detector (Showa Denko KK, Kawasaki, Japan). The mobile phase used was 0.2 M $NaNO_3$ and the column temperature was set to 55 °C. The flow rate was 0.6 mL/min (isocratic elution). The injection volume was 10 μL. The system was calibrated using a pullulan series of known molecular weights (Sigma-Aldrich).

2.7. *Oligosaccharide profiling by HPAEC-PAD*

Oligosaccharide profiles of supernatants at the end of *in vitro* AIS digestion (480 min; see Section 2.3.1) were investigated by HPAEC-PAD using the same equipment as mentioned above, as previously described (Kouzounis et al., 2022). The mobile phases used were 0.1 M sodium hydroxide (NaOH) (A) and 1 M sodium acetate in 0.1 M NaOH (B). The

flow rate was 0.3 mL/min. The separation was performed by using the following elution profile: 0–32 min from 0 % to 38 % B (linear gradient), 32–37 min from 32 % to 100 % B, 37–42 min at 100 % B (isocratic), 42–42.1 min to 100 % A (linear gradient) and 42.1–55 min 100 % A (isocratic). Analytical standards were used for the identification of Glc, Rib, cellobiose and linear xylo-oligosaccharides. AXOS were identified based on the elution pattern of reference AXOS prepared from wheat flour AX after hydrolysis with a pure GH11 *endo*-xylanase (see supplement 1.6).

2.8. Oligosaccharide profiling by MALDI-TOF-MS

Oligosaccharide profiles of supernatants at the end of *in vitro* AIS digestion (480 min; see Section 2.3.1) were investigated by matrix-assisted laser desorption/ionization time-of-flight mass spectrometry using an autoflex® maX MALDI-TOF mass spectrometer (Bruker Daltonics Inc., Billerica, MA, USA). The equipment was controlled with a flexControl 3.4 software and operated in positive mode. The mass spectrometer was calibrated with maltodextrins (Avebe, Veendam, the Netherlands) in a mass range of *m/z* 500–3500. In addition, the presence of ester-bound ferulic acid moieties was evaluated by performing MALDI-TOF-MS without and with alkali treatment as described by Appeldoorn et al. (2010), with several modifications. Briefly, 25 μL supernatant was mixed with 25 μL 0.5 N KOH and was incubated for 16 h at 4 °C. The samples were then acidified by the addition of 25 μL 0.5 N acetic acid. Next, 175 μL water was added to achieve a tenfold dilution of the original sample. Non-saponified supernatants were diluted ten times directly in water. The final samples were desalted with Dowex 50 W-X8 resin (Sigma-Aldrich) and 1 μL aliquot was co-crystallized with matrix solution (1 μL; 25 mg/mL di-hydroxy-benzoic acid (Sigma-Aldrich)) in 50 % (v/v) acetonitrile (VWR International B.V., Amsterdam, the Netherlands) on a target plate, under a stream of dry air.

2.9. Scanning electron microscopy (SEM)

The microstructure of undigested cereal grains was analyzed by SEM, according to Klostermann et al. (2023). Aliquots of the slurry obtained at the end of *in vitro* digestion of whole grains (see Section 2.3.2) were dried on Whatman® Nuclepore™ membranes (diameter 13 mm, pore size 10 μm; Merck Life Science B.V., the Netherlands) in a flow cabinet and was subsequently attached to sample holders containing carbon adhesive tabs (EMS, Washington, USA) and coated with 12 nm tungsten (EM SCD 500, Leica, Vienna, Austria). The samples were analyzed with scanning electron microscopy (SEM) (Magellan 400, FEI, Eindhoven, The Netherlands) at the Wageningen Electron Microscopy Center (WEMC). SEM images were recorded at an acceleration voltage of 2 kV and 13 pA and magnification of 1000 times (ETD detector). At least 25 images were recorded for each sample.

2.10. Calculations

2.10.1. Carbohydrate release from AIS by HX and EG7 under in vitro digestion conditions

The amount of carbohydrates (CHO_R: AX (sum of Ara and Xyl), Glc, Gal and Man) released at time t during *in vitro* digestion of AIS without or with enzyme addition was expressed as a percentage (% w/w) of the respective carbohydrate in AIS (see supplement 1.4):

$$CHO_R\ (t) = \frac{C(t)*V(t)}{m_{AIS}*\left(\frac{C_{CHO}}{100}\right)} \quad (1)$$

where, C(t) is the anhydro sugar concentration (mg/mL) measured in the supernatant and V(t) is the volume (mL) of solution during *in vitro* digestion, corrected for the volume of supernatant removed during sampling, m_{AIS} is the amount (mg) of AIS in the reaction tube and C_{CHO} is the content (% w/w) of each carbohydrate in AIS.

2.10.2. In vitro starch digestion

The amount of hydrolyzed starch at time t was expressed as a percentage (HS, % w/w) of the total starch present in whole grains:

$$HS\ (t) = \frac{C(t)*V(t)}{m_{grain}*\left(\frac{C_{STA}}{100}\right)} \quad (2)$$

where, C(t) is the anhydro Glc concentration (mg/mL) measured in the supernatant and V(t) is the volume (mL) of solution, corrected for soluble starch content after 60 min in the gizzard phase (Table S2) and the volume of sampled supernatant during *in vitro* digestion, m_{grain} is the amount (mg) of whole grain in the reaction tube and C_{STA} is the total starch content in grains (% w/w).

2.11. Mathematical modelling of in vitro starch digestion

The hydrolyzed starch HS(t) (%) at a digestion time t (min) was modelled using the Chapman-Richards model (van Kempen et al., 2007, 2010):

$$HS\ (t) = HS_{max}\ (1 - exp(-kt))^n \quad (3)$$

where, HS_{max} is the maximum released starch (%), k is the rate of starch hydrolysis (%/min), n is the shape parameter (dimensionless), and t is the digestion time (min).

First, the model (Eq. (3)) required estimating 3 parameters: HS_{max}, k, and n calculated by a global optimisation using MATLAB 2021b software (Mathworks, Natick, MA, USA). Typically, the optimization requires starting values of 3 parameters which we obtained from previous research (van Kempen et al., 2010). Then, for every set of initial starting values, the final estimated values were determined by minimizing the difference between experimental and theoretical data obtained for HS(t) (Eq. (3)), using the *'lsqnonlin'* algorithm of the MATLAB software. Since each set of starting values returned different estimated values, the optimal estimated values were selected based on the least squared error. Second, after fitting the numerical and experimental datasets, Monte Carlo simulations with 200 iterations were performed to evaluate the uncertainty in the estimation (Nguyen et al., 2024; van Boekel, 2008). Finally, the Root Mean Square Error (RMSE) values between the experimental and numerical data were calculated to evaluate the model fitting.

2.12. Statistical analysis

The data obtained was subjected to analysis of variance (ANOVA) using R version 4.2.1. The impact of enzyme treatment on carbohydrate release at the end of *in vitro* digestion (480 min) was modelled separately for wheat and maize AIS. The impact of treatment on HS_{max}, k, and n parameters estimated for starch digestion was modelled for both grains. Normality of data residuals and homogeneity of variance were additionally checked. To test the significance of the differences between treatments, Tukey's post-hoc test was performed, with a significance threshold set at $P < 0.05$.

3. Results and discussion

3.1. Chemical composition of whole grains and AIS

Cell wall polysaccharides from wheat and maize whole grains were isolated as alcohol insoluble solids (AIS) (Table 1). The isolation procedure resulted in two carbohydrate-rich fractions (AIS: 60.1 and 57.3 % w/w carbohydrates; Table 1), representing 15.0 % and 16.8 % of the starting dry matter for wheat and maize, respectively. Arabinoxylan (AX) was the main NSP present in both wheat AIS (W-AIS AX: 37.6 % w/

Table 1
Chemical composition (% w/w, dry matter) of wheat and maize whole grains and chemical composition and yield of wheat (W-AIS) and maize AIS (M-AIS). The analytical methods followed for the proximate compositional analysis of whole grains and AIS are described in Supplement 1.1.

	Wheat whole grain	W-AIS	Maize whole grain	M-AIS
Dry matter (% total solids)	89.6 ± 0.1	95.7 ± 0.2	89.7 ± 0.0	95.9 ± 0.5
Yield (% grain DM)	–	15.0	–	16.8
Ash	1.8 ± 0.0	5.1 ± 0.0	1.3 ± 0.1	4.7 ± 0.1
Protein (N × 5.7)	13.3 ± 0.6	24.3 ± 0.3	7.5 ± 0.3	32.4 ± 1.3
Total carbohydrates	82.3 ± 2.1	60.1 ± 2.2	89.5 ± 1.5	57.3 ± 2.6
Starch	64.9 ± 1.8	1.2 ± 0.3	75.7 ± 1.4	3.5 ± 0.2
Arabinoxylan[a]	7.6 ± 0.3	37.6 ± 1.5	4.3 ± 0.4	28.6 ± 2.0
Glc	72.2 ± 2.1	16.6 ± 0.7	82.2 ± 1.9	19.8 ± 0.8
Gal	0.6 ± 0.0	1.6 ± 0.0	0.7 ± 0.1	3.0 ± 0.2
Man	0.5 ± 0.1	1.3 ± 0.0	0.1 ± 0.0	0.9 ± 0.1
UA	1.4 ± 0.1	2.9 ± 0.1	1.8 ± 0.1	4.7 ± 0.0
Ara/Xyl (mol/mol)	0.61 ± 0.02	0.60 ± 0.02	0.74 ± 0.04	0.67 ± 0.03

[a] Sum of arabinosyl and xylosyl units.

w) and maize AIS (M-AIS AX: 28.6 % w/w). Non-starch Glc, mainly representing cellulose (Bach Knudsen, 2014), accounted for 15.4 % (w/w) for W-AIS and 16.3 % (w/w) for M-AIS (Table 1). Uronic acids (UA) were present at 2.9 % (w/w) and 4.7 % (w/w) in W-AIS and M-AIS, respectively. UA may represent galacturonic acid as a building block of pectin present in low amounts in cereal grains, but also glucuronic acid present as substituent of glucurono-AX (GAX) (Fincher & Stone, 2004). Lastly, Gal and Man were expected to derive from other NSP, such as glucomannan and arabinogalactan (Fincher & Stone, 2004; Tryfona et al., 2010).

3.2. Cell wall NSP degradation by endo-xylanase and endo-glucanase during in vitro digestion

The first aim of this study was to monitor the degradation of W-AIS and M-AIS by *endo*-xylanase (HX) and *endo*-glucanase (EG7) under *in vitro* conditions mimicking the poultry digestive tract, in order to investigate the efficacy of NSPases as dietary supplements for broilers. HX is a commercial enzyme containing primarily a GH11 *endo*-xylanase, but also exhibiting glucanase activity (Table S1). EG7 was chosen for its ability to degrade cellulose as well as β-(1 ➔ 3,1 ➔ 4)-linked glucan (MLG), both of which are found in cereal grains (Bach Knudsen, 2014; Karlsson et al., 2002; Vlasenko et al., 2010). The previously reported side-activity of GH7 *endo*-glucanases on (arabino)xylans (Vlasenko et al., 2010) was currently confirmed for EG7 (Table S1). Feed retention in the poultry GIT is typically around 3 h (Svihus & Itani, 2019). Currently, *in vitro* AIS digestion was followed for 480 min. The prolonged *in vitro* digestion aimed at determining the potential "end-point" of HX and EG7 action. This approach aims at investigating in detail the extent of NSP hydrolysis by feed enzymes, under digestive conditions, and not at fully simulating feed digestion.

Solubilization of total carbohydrates under *in vitro* digestion conditions for untreated (Untr) and HX and EG7 treated W-AIS and M-AIS is presented in Fig. 1. W-AIS presented a higher proportion of soluble carbohydrates compared to M-AIS (Untr; 9.6 % *vs* 3.4 %), reflecting the different content of soluble NSP found in wheat and maize grains. It is widely accepted that differences in NSP solubility between cereals is related to their fine chemical structure (*e.g.* degree of substitution, molecular weight) as well as to cross-linking within the cell wall matrix (Bach Knudsen, 2014). The carbohydrate fraction solubilized during *in vitro* digestion of Untr samples is expected to mainly represent water-

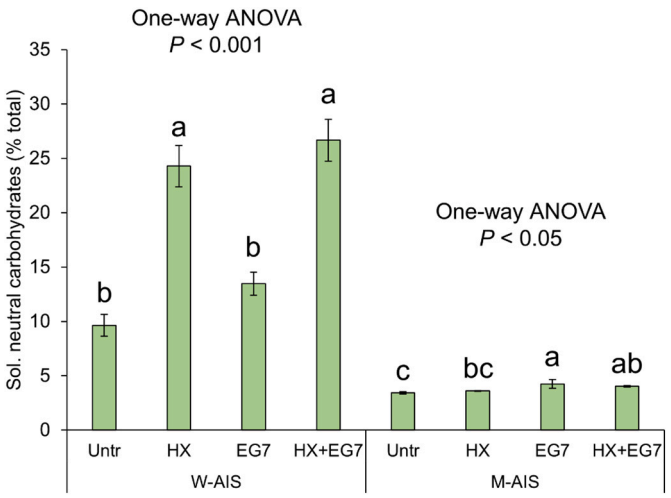

Fig. 1. Soluble neutral carbohydrates (sum of Ara, Xyl, Glc, Man and Gal units) release expressed as percentage (%) of total neutral carbohydrates, after 480 min of *in vitro* digestion of W-AIS and M-AIS without enzyme addition (Untr) or with the addition of HX, EG7 and HX + EG7. Bars corresponding to W-AIS or M-AIS not sharing common letter notation differ significantly ($P < 0.05$). The error bars indicate standard deviation ($n = 3$). ANOVA results are presented above the bars.

soluble polysaccharides present in AIS (Kabel et al., 2002). It is clear from Fig. 1 that enzyme treatment resulted in additional carbohydrate release from both substrates at the end of *in vitro* digestion. The combined *endo*-xylanase and *endo*-glucanase treatment (HX + EG7) increased the amount of soluble carbohydrates by 2.8 times in W-AIS and 1.2 times in M-AIS, compared to the corresponding Untr. In particular, HX and HX + EG7 treatments increased the amount of soluble carbohydrates from W-AIS to a similar extent, while EG7 released carbohydrates from M-AIS to a greater extent than HX. Next, a closer examination on the action of HX and EG7 on AX and glucans was undertaken.

3.2.1. AX degradation by endo-xylanase is predominant for wheat AIS

The release of AX and Glc residues from W-AIS during *in vitro* digestion is presented in Fig. 2A and B, respectively. It was observed that 14.1 % AX and 7.5 % Glc units in W-AIS were solubilized during the gizzard phase (Gi) without enzyme addition (Untr). Hardly any subsequent NSP solubilization for Untr in the small intestine (SI) phase was observed (Fig. 2), as previously reported (Vangsøe et al., 2021). Enzyme addition resulted in both AX and Glc units release by the end of *in vitro* digestion ($P < 0.05$). In particular, HX released 17.0 % AX by the end of the Gi phase (60 min). AX release by HX became more pronounced during the SI phase. For instance, 25.3 % AX was soluble at 90 min (total digestion time) while 29.7 % AX was released at the end of *in vitro* digestion (480 min). W-AIS incubation with EG7 also resulted in AX release in SI, albeit to a lower extent than HX ($P < 0.05$). Finally, HX + EG7 released a similar proportion of AX during both Gi and SI compared to HX ($P > 0.05$). The enzymatic degradation of Glc-containing NSP proceeded differently to that of AX. When added alone, HX and EG7 released 12.3 % and 11.4 % Glc units from W-AIS (480 min), respectively, both being already higher ($P < 0.05$) than Untr (8.0 %). However, HX + EG7 combination released much more Glc (18.1 %) than the individual enzymatic treatments ($P < 0.05$).

The increase of soluble carbohydrates (Fig. 2A, B) and the large amounts of released AX (Table S3) pointed clearly to the solubilization of insoluble AX from the cell wall by HX, EG7 and HX + EG7. AX solubilization was accompanied by a gradual reduction of arabinose-to-xylose ratio (Ara/Xyl) of the soluble AX material (Fig. 2C). Ara/Xyl ratios of 0.7–0.8 were obtained for Untr and EG7 and ~0.6 for both HX and HX + EG7, at the end of *in vitro* digestion, pointing to the release of

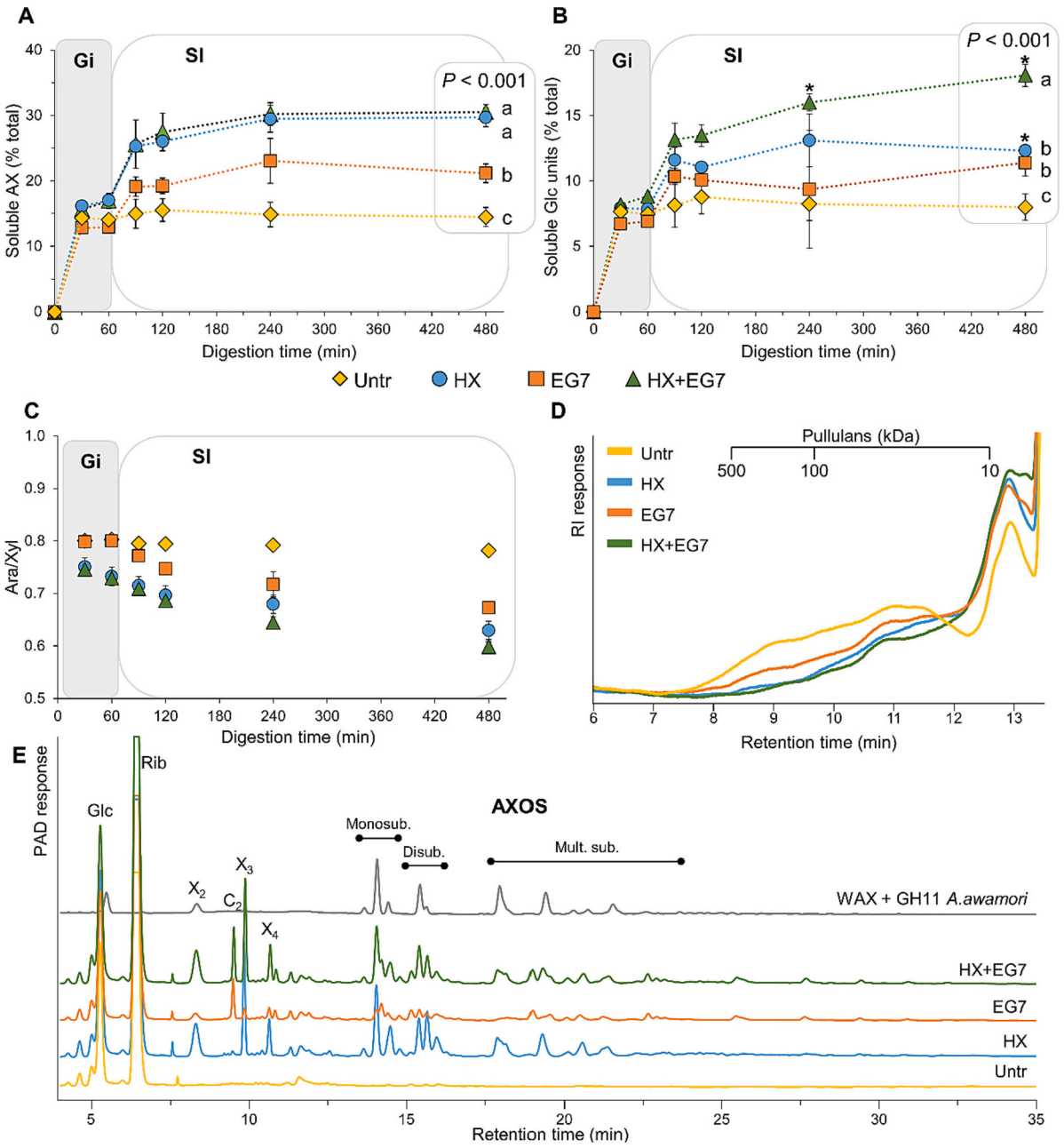

Fig. 2. Arabinoxylan (**A**) and glucose units (**B**) release, expressed as percentage (%) of total AX or Glc, and arabinose-to-xylose ratio (Ara/Xyl) of released AX (**C**) during incubation of W-AIS under *in vitro* digestive conditions without enzyme addition (Untr: ◆) or with the addition of HX (●), EG7 (■) and HX + EG7 (▲). The error bars indicate standard deviation ($n = 3$, except for $^*n = 2$). The significance of enzyme addition on carbohydrate release at the end of *in vitro* digestion (480 min) was assessed by one-way ANOVA, followed by Tukey's HSD test ($P < 0.05$). Values not sharing common letter notation differ significantly. HPSEC-RI elution patterns (**D**) of supernatants obtained after 480 min of *in vitro* digestion. Pullulan standards were used as calibrants. HPAEC-PAD chromatograms (**E**) of supernatants obtained after 480 min of *in vitro* digestion. Glucose (Glc), ribose (Rib), xylobiose (X_2), xylotriose (X_3), xylotetraose (X_4) and cellobiose (C_2) were labelled according to analytical standards; AXOS were grouped in monosubstituted, disubstituted and multiple-substituted oligosaccharides (van Gool et al., 2013), using as reference the AXOS profile generated upon wheat arabinoxylan degradation by GH11 *endo*-xylanase from *A. awamori* (see supplement 1.6); # peaks disappearing upon treatment with lichenase (*endo*-1,3,1,4-β-D-glucanase) from *B. subtilis* (data not shown); Gi: gizzard phase, SI: small intestine phase.

relatively low-substituted AX.

Monitoring the molecular weight (Mw) distribution of soluble components by HPSEC-RI (Fig. 2D) revealed that enzyme action degraded soluble polymeric AX and released insoluble AX as low Mw material at the end of *in vitro* digestion. This observation was consistent with the formation by HX of DP 2–4 xylo-oligosaccharides (XOS) and differently substituted AXOS at the end of *in vitro* digestion, as determined by HPAEC (Fig. 2E). Mono-, di- and multiple-substituted AXOS released by HX were annotated according to the elution pattern of AXOS released by a reference GH11 *endo*-xylanase (van Gool et al., 2013). EG7 released cellobiose and other oligosaccharides eluting in the same retention time range as AXOS. HX + EG7 treatment released a combination of oligosaccharides that were released by individual HX and EG7 treatments. For both EG7 and HX + EG7 treatments, the unknown peaks eluting after 19 min not corresponding to DP 3–7 cellodextrins (RT 10–15 min) or reference AXOS were assigned to mixed-linkage gluco-oligosaccharides (Fig. 2E; peaks annotated with "#"). This was achieved by incubating the supernatant from HX + EG7 treatment (480 min) with

lichenase and monitoring changes in the oligosaccharide profile by HPAEC (data not shown). Gluco-oligosaccharide formation was consistent with the release of Glc units (Fig. 2B) but not of Man or Gal units (Fig. S3). The presence of Glc as free monomer in all treatments (Fig. 2E) was mainly attributed to incomplete starch-derived Glc removal during AIS isolation, whereas <1 % of total Glc was released as monomer after 480 min, for all treatments (data not shown).

MALDI-TOF-MS analysis of the soluble fraction after 480 min of *in vitro* digestion was performed to further study the profile of oligosaccharides generated upon treatment by HX, EG7 and HX + EG7 (Fig. 3). All enzyme treatments predominantly released a homologous series corresponding to DP 5–26 pentose oligomers (sequential increments of *m/z* 132; $P_{5–26}$), representing (A)XOS. Next, the series of DP 4–17 hexose oligomers (sequential increments of *m/z* 162; $H_{4–17}$) was mainly released by EG7 and HX + EG7 treatments, representing hydrolytic products originating from cellulose and/or MLG, thus confirming the HPAEC data (Fig. 2E). In addition, DP 6–10 AXOS with an additional *m/z* 176 moiety that were released after HX and HX + EG7 treatments, were identified as feruloylated AXOS. Their identification was inferred by the disappearance of the corresponding MALDI-TOF-MS peaks upon saponification (Fig. S4), indicating the release of the esterified ferulic acid moiety (Appeldoorn et al., 2010).

Our findings indicated that dietary enzyme action began by depolymerizing soluble AX in the gizzard. This is supported by the limited AX solubilization observed during Gi, as can be seen by the similar amounts released after 30 and 60 min of *in vitro* digestion (Fig. 2A). At the same time, enzyme action during Gi was able to depolymerize soluble polymers, as determined by HPSEC analysis (Fig. S5). These findings are in agreement with recent *in vivo* and *in vitro* studies reporting that AX degradation by dietary *endo*-xylanase in the broiler gastrointestinal tract (GIT) began in the early stages of digestion (Deshors et al., 2019; Kouzounis et al., 2022; Matthiesen et al., 2021). AX and Glc units release by NSPases became more pronounced under SI conditions. This observation was in line with the increased activity of GH11 *endo*-xylanases and GH7 *endo*-glucanases from *Trichoderma sp.* under pH conditions similar to that of SI (Becker et al., 2001; Paës et al., 2012).

The combined xylanase/glucanase supplementation was previously found to release ~40 % of xylose from wheat grains *in vitro* (Vangsøe et al., 2021). The soluble AX values of 21.1–30.5 % currently obtained upon enzyme treatment were somewhat lower, but were comparable with the proportion of soluble AX (20–27 % of total AX) present in the ileum of broilers fed xylanase-supplemented wheat diets (Bautil et al., 2021; Kouzounis et al., 2022). It should be mentioned that the amount of *endo*-xylanase added per g NSP was estimated to be ~14 times higher in this study than in a previous *in vivo* study, where *endo*-xylanase was added at 1500 xylanase units (EPU; Table S1) per kg feed (Kouzounis et al., 2021). Interestingly, the HX and EG7 combination improved glucan but not AX release from W-AIS, despite the xylan-degrading capability of EG7 (Vlasenko et al., 2010). The increased Glc units release was most likely attributed to the combined action of EG7 and glucanases present in HX. A potential synergism between *endo*-xylanase and *endo*-glucanase would have resulted in higher release of both AX and Glc units (Song et al., 2016).

The (A)XOS profile currently obtained by HX was in line with the GH11 *endo*-xylanase mode of action (Paës et al., 2012). The release of mainly XOS and relatively low-substituted (mono-, di-) AXOS coincided with the decreased Ara/Xyl ratio values of solubilized AX material (Fig. 2 C,E), pinpointing that GH11 *endo*-xylanase mainly acted on low-substituted AXs. Such AXs are mainly found in the *endo*sperm and aleurone and hyaline layers, and are more susceptible to *endo*-xylanase compared to highly-substituted AXs found in the outer pericarp (Barron et al., 2007; Benamrouche et al., 2002; Vangsøe et al., 2021). The release of both (A)XOS and feruloylated AXOS (Fig. 3; Fig. S4) suggested that NSPases attacked cell walls from various grain tissues, as AXs present in

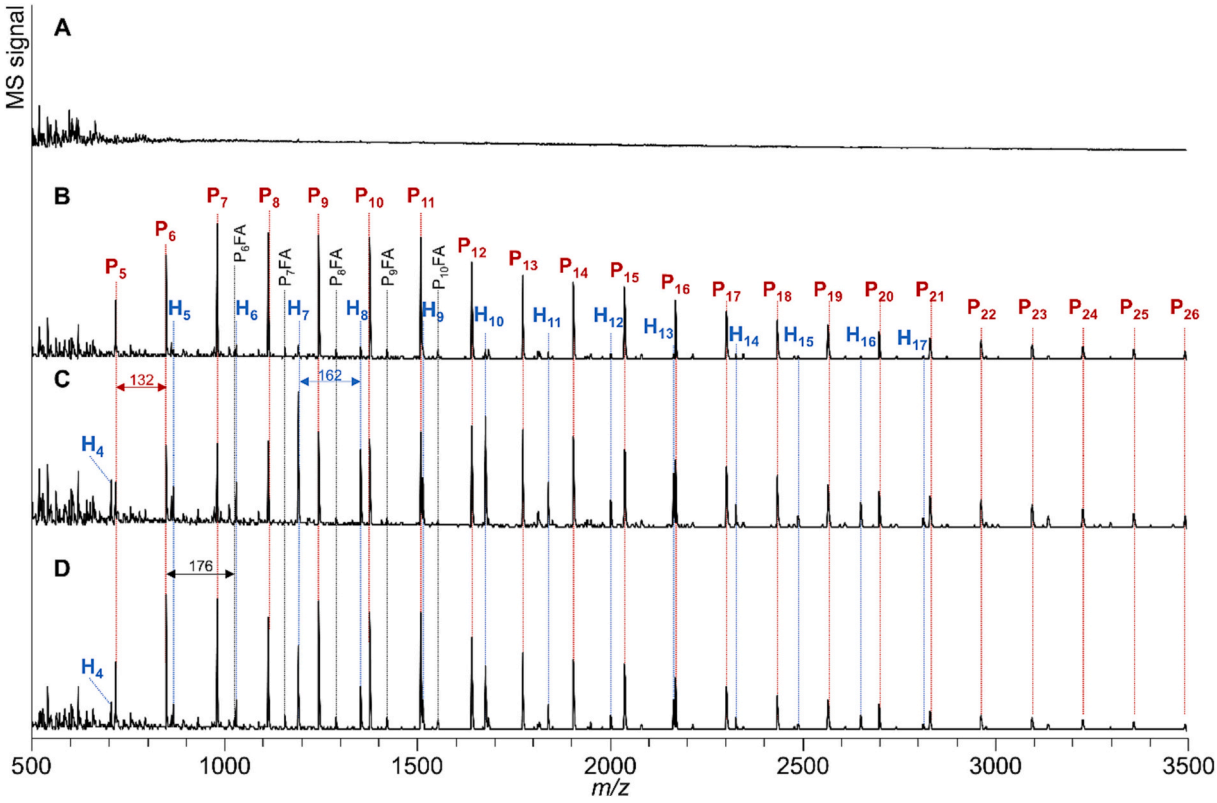

Fig. 3. MALDI-TOF mass spectra (*m/z* 500–3500) of supernatants obtained after 480 min of *in vitro* digestion of W-AIS without enzyme addition (Untr: **A**) or with the addition of HX (**B**), EG7 (**C**) and HX + EG7 (**C**). The peaks were tentatively annotated: P; pentose, H; hexose, FA; ferulic acid. The mass difference (Da) between peaks is provided.

the peripheral layers are typically more substituted by ferulic acid compared to *endo*sperm AX (Barron et al., 2007; Marcotuli et al., 2016).

3.2.2. Enzyme action released diverse NSP structures from maize AIS

The solubilization of AX and Glc units was also monitored *in vitro* during the enzymatic treatment of M-AIS (Fig. 4). The low proportions of soluble AX and Glc observed for M-AIS were consistent with the lower carbohydrate solubility, compared to W-AIS (Fig. 1). Moreover, the fluctuation in solubilized AX values observed between 240 and 480 min is expected to have been caused by the low amounts of solubilized AX (Fig. 4A), and a similar behavior was not observed for the more abundantly present Glc units (Fig. 4B). EG7 treatment with and without HX was found to solubilize both AX and Glc, while HX treatment only marginally affected NSP release. In specific, EG7 and HX + EG7 treatments presented 7.3 % and 7.0 % soluble Glc units after 480 min of *in vitro* digestion, respectively, which were significantly higher than the values obtained for Untr (5.7 %) and HX (6.0 %) ($P < 0.05$). AX release was documented for all enzyme treatments, with the values obtained for EG7 (2.1 %) and HX + EG7 (2.2 %) being significantly higher than the values for Untr (1.3 %) and HX (1.6 %) ($P < 0.05$). Next to AX and Glc, EG7 and HX + EG7 also released Gal (4.7–5.0 %) units from M-AIS, but not Man (Fig. S3). EG7 and HX + EG7 released Glc, cellobiose and larger oligosaccharides that did not correspond to (A)XOS or cellodextrins, as determined by HPAEC (Fig. 4C).

The low AX solubilization reflected the recalcitrance of heavily substituted maize AXs to hydrolysis by GH11 *endo*-xylanases (Paës et al., 2012). A previous *in vitro* study reported considerably higher hydrolysis of maize AX by using thousandfold higher dose of xylanase/glucanase compared to the corresponding treatment of wheat substrates (Vangsøe et al., 2021). In our study, by using similar enzyme concentration as for W-AIS, we observed NSPase-mediated release of various NSP from M-AIS. Based on the sugar composition of M-AIS (Table 1), it was determined that the increase in soluble Glc units by 23–29 % upon HG + EG7 and EG7 treatments of M-AIS (Fig. 4B) was a main contributor in the overall NSP solubilization from this substrate (Fig. 1). These findings indicated the importance of *endo*-glucanase for maize NSP hydrolysis and were partly in line with studies demonstrating the beneficial impact of xylanase/glucanase or multi-enzyme combinations for broiler growth (Cowieson et al., 2010; Meng et al., 2005). Nevertheless, the high nutritive value of maize alongside the seemingly low release of readily fermentable NSP from maize, especially within the constraints of the poultry GIT, are expected to limit the response of maize-fed broilers towards NSPases (Cowieson et al., 2010; Sanchez et al., 2021). It could be envisaged that the inclusion of AX-debranching enzymes (*i.e.* arabinofuranosidases, feruloyl esterases, α-glucuronidases) in *endo*-xylanase/*endo*-glucanase preparations could increase oligosaccharide release from maize (Dodd & Cann, 2009; Ravn et al., 2018).

3.3. Impact of cell wall NSP degradation by endo-xylanase and endo-glucanase on grain microstructure and in vitro starch digestion kinetics

The impact of cell wall degradation by NSPases on the nutritive value of cereal was further investigated by *in vitro* digestion of wheat and maize grains. It should be noted that the cell wall material-to-enzyme ratio used during *in vitro* digestion of grains was double compared to the one used during *in vitro* digestion of isolated cell wall material (AIS). This enzyme dose was estimated to be ~28 times higher the one used previously *in vivo* (Kouzounis et al., 2021), and was chosen to ensure

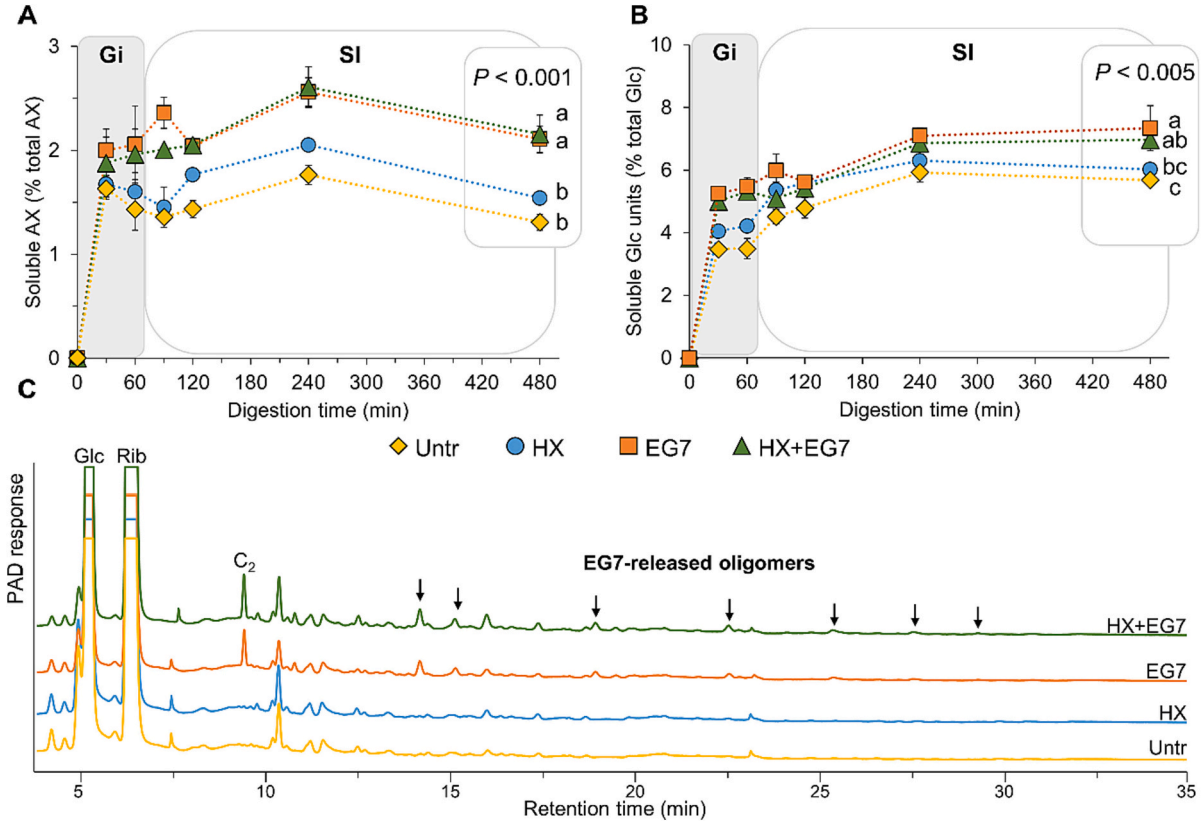

Fig. 4. Arabinoxylan (**A**) and glucose units (**B**) release, expressed as percentage (%) of AX or total Glc during incubation of M-AIS under *in vitro* digestive conditions without enzyme addition (Untr: ◇) or with the addition of HX (○), EG7 (□) and HX + EG7 (△). The error bars indicate standard deviation ($n = 3$). The significance of enzyme addition on carbohydrate release at the end of *in vitro* digestion (480 min) was assessed by one-way ANOVA, followed by Tukey's HSD test ($P < 0.05$). Values not sharing common letter notation differ significantly. HPAEC-PAD elution patterns (**C**) of supernatants obtained after 480 min of *in vitro* digestion. Glucose (Glc), ribose (Rib) and cellobiose (C_2) were labelled according to analytical standards. Gi: gizzard phase, SI: small intestine phase.

extensive NSP degradation. Such enzyme dose was chosen to determine the potential of feed enzymes, under *in vitro* digestive conditions, to influence starch digestion kinetics by offsetting the encapsulating effect of the cell wall matrix, and not to fully mimic the enzymes levels used in *in vivo* studies (Bedford, 2018). Having established the extent and profile of enzymatic action on AIS isolated from the same grains in the previous sections, we now focused on grain microstructure and starch digestion kinetics.

3.3.1. Grain microstructure at the end of in vitro digestion

The microstructure of grains was examined at the end of *in vitro* digestion by SEM (Fig. 5). Cell walls from the endosperm, aleurone and pericarp could be visualized in the undigested residues, as confirmed by comparison with previous research (Gartaula et al., 2017). Wheat *endo*sperm images (Fig. 5B, E, D) demonstrated the scarce presence of intact starch granules at the end of *in vitro* digestion. In contrast, maize *endo*sperm images presented a more abundant presence of partially digested starch granules, as visualized by the presence of several pores on the granules (Fig. 5F, G). *Endo*-xylanase and *endo*-glucanase treatment (W-HX + EG7) appeared to influence the microstructure of wheat grains, as demonstrated by the presence of damaged cell walls (Fig. 5E). Cell wall degradation was visualized by the presence of punctures on the surface. Similar microstructure was not observed for W-Untr (Fig. 5A, B, C), indicating that such puncturing of the cell walls was caused by NSPases. SEM observations were in line with AX and Glc unit release from wheat AIS (Fig. 2) and further documented the degradation of insoluble cell walls by feed enzymes. The low amount of enzymatically-released NSP upon HX + EG7 treatment of M-AIS correlated with a visually similar microstructure of maize grains without (M-Untr) and with HX + EG7 treatment (M-HX + EG7) (Fig. 5F, G). Overall, the co-presence and arrangement of different types of grain tissue indicated a low degree of grain intactness that made it cumbersome to deduce the identity of damaged cell walls by SEM imaging. Nevertheless, these findings underlined that NSPase action on insoluble NSP, as evaluated for AIS *in vitro*, resulted in the partial dismantling of cell walls in whole grains.

3.3.2. In vitro starch digestion kinetics

The cell wall matrix has been widely considered as a physical barrier that hinders nutrient digestion (Bhattarai et al., 2018; Grundy et al., 2022). Hence, we evaluated the possible implications of cell wall degradation by NSPases for *in vitro* starch digestion. Starch digestion is often assessed *in vitro* with the model introduced by Englyst and co-workers to classify starch into digestible and resistant fractions, with or without modifications (Englyst et al., 1992; Martens et al., 2018; van Kempen et al., 2010). However, the suitability of this approach for kinetic studies is questionable due to the simultaneous addition and excessive amounts of α-amylase and fungal amyloglucosidase (Weurding et al., 2001). In specific, the synergy exhibited by the high levels of these two enzymes towards starch granules may not be entirely representative of digestive processes in the mammalian and fowl GIT (Brownlee et al., 2018; Hernandez-Hernandez et al., 2019; Warren et al., 2015; Zaefarian et al., 2015). In our approach, *in vitro* grain digestion was carried out by pepsin during the gizzard phase, followed by pancreatin during the small intestine phase. The pancreatin-to-starch weight ratio used was tenfold lower than that reported in studies employing the Englyst model (Martens et al., 2018; van Kempen et al., 2010). Preliminary experiments using the same cereal grains as in the present study indicated that the final pancreatin dose was sufficient for starch digestion to reach a plateau under the current experimental conditions (data not shown). This approach allowed the accurate estimation of the maximum released starch (HS_{max}), which is essential for the accurate and precise modelling of starch digestion kinetics. It should be mentioned that even lower (~20–50 times) pancreatin-to-starch weight ratios have been used in studies using different *in vitro* digestion models (Bustos et al., 2017; Tervilä-Wilo et al., 1996). Currently, fungal amyloglucosidase was added to supernatant aliquots sampled during *in vitro* digestion. This was done to convert hydrolyzed starch to easily quantifiable Glc, and not to mimic the action of brush border α-glucosidases. Still, it certainly is acknowledged that both α-amylase and α-glucosidases do contribute to starch digestion (Hernandez-Hernandez et al., 2019). The modifications introduced here aim at the mechanistic understanding of the potential impact of NSPases on starch hydrolysis, and not at fully simulating gastrointestinal digestion.

The kinetic curves of *in vitro* starch digestion are shown in Fig. 6 and Table 2. The mathematical model fitted well with the experimental data, as seen by the RMSE values lower than 1.0 (Table 2). The higher *in vitro* starch digestibility observed for wheat compared to maize was in line with SEM observations (Fig. 5) and even comparable with previous research on isolated starches (Martens et al., 2018). The estimated maximum starch digestibility values (HS_{max}) of 56.3–57.0 % and 44.6–45.8 % obtained for wheat and maize, respectively, were considerably lower than in previous *in vitro* studies (Martens et al., 2018; Weurding et al., 2001), most likely due the type and amount of amylolytic enzymes used. Furthermore, the current HS_{max} values do not represent the ileal starch digestibility values above 80 % obtained for broilers *in vivo*, for both wheat and maize diets (Zaefarian et al., 2015). It should be emphasized that our aim was to investigate the implications of cell wall degradation by NSPases on starch digestion kinetics, and not to fully mimic feed digestion by poultry.

For the same grain type, Untr and HX + EG7 presented similar curve shapes and similar HS_{max} and k values ($P > 0.05$; Table 2), indicating that cell wall hydrolysis did not impact the extent or rate of *in vitro* starch digestion in the current study. The shape parameter n is related to the lag phase of *in vitro* starch digestion (van Kempen et al., 2007). High n values indicate a long lag phase which has been associated with decreased starch accessibility by amylolytic enzymes (van Kempen et al., 2007). Although no significant effect of enzyme treatment could be discerned, the n values close to zero across all treatments suggested that the lag phase for starch hydrolysis was minute in the current experiments (van Kempen et al., 2007, 2010). Overall, the kinetic parameters currently estimated were in line with previously reported trends, even though the type and amount of amylolytic enzymes used resulted in underestimation of *in vitro* starch digestibility (Martens et al., 2018; van Kempen et al., 2007, 2010). That being said, the present approach is considered suitable for monitoring *in vitro* the potential impact of NSPases on starch digestion kinetics.

3.4. Degradation of cell wall polysaccharides in the context of improving feed utilization

NSPases such as *endo*-xylanase and *endo*-glucanase are typically added as supplements in broiler diets. This practice is associated with improved productive performance and gut health and with decreased feed costs (Bedford, 2018; Pan & Yu, 2013). Our study demonstrated that dietary *endo*-xylanase depolymerized soluble NSP in the early stages of *in vitro* digestion. Such action is expected to be linked with lower intestinal viscosity and improved nutrient digestibility observed *in vivo* (Choct & Annison, 1992). The impact of NSPases on viscosity was not currently assessed due to the lower solid content of *in vitro* digesta (1–3 %) compared to the broiler small intestine (~18 %) (Morgan et al., 2019).

NSPases proceeded to release readily fermentable oligosaccharides from insoluble NSP fractions under *in vitro* conditions simulating the small intestine. For wheat AIS, AX degradation by *endo*-xylanase was more extensive than that of glucans (MLG, cellulose) by *endo*-glucanase (Fig. 2). Nevertheless, both enzymes released oligosaccharides with diverse structures. Consequently, it is demonstrated that both *endo*-xylanase and *endo*-glucanase contribute to the degradation of insoluble NSP originating from various wheat grain tissues. W-AIS was more susceptible to enzymatic degradation compared to M-AIS (Figs. 1, 4), in line with previous *in vivo* and *in vitro* studies (Kouzounis et al., 2021;

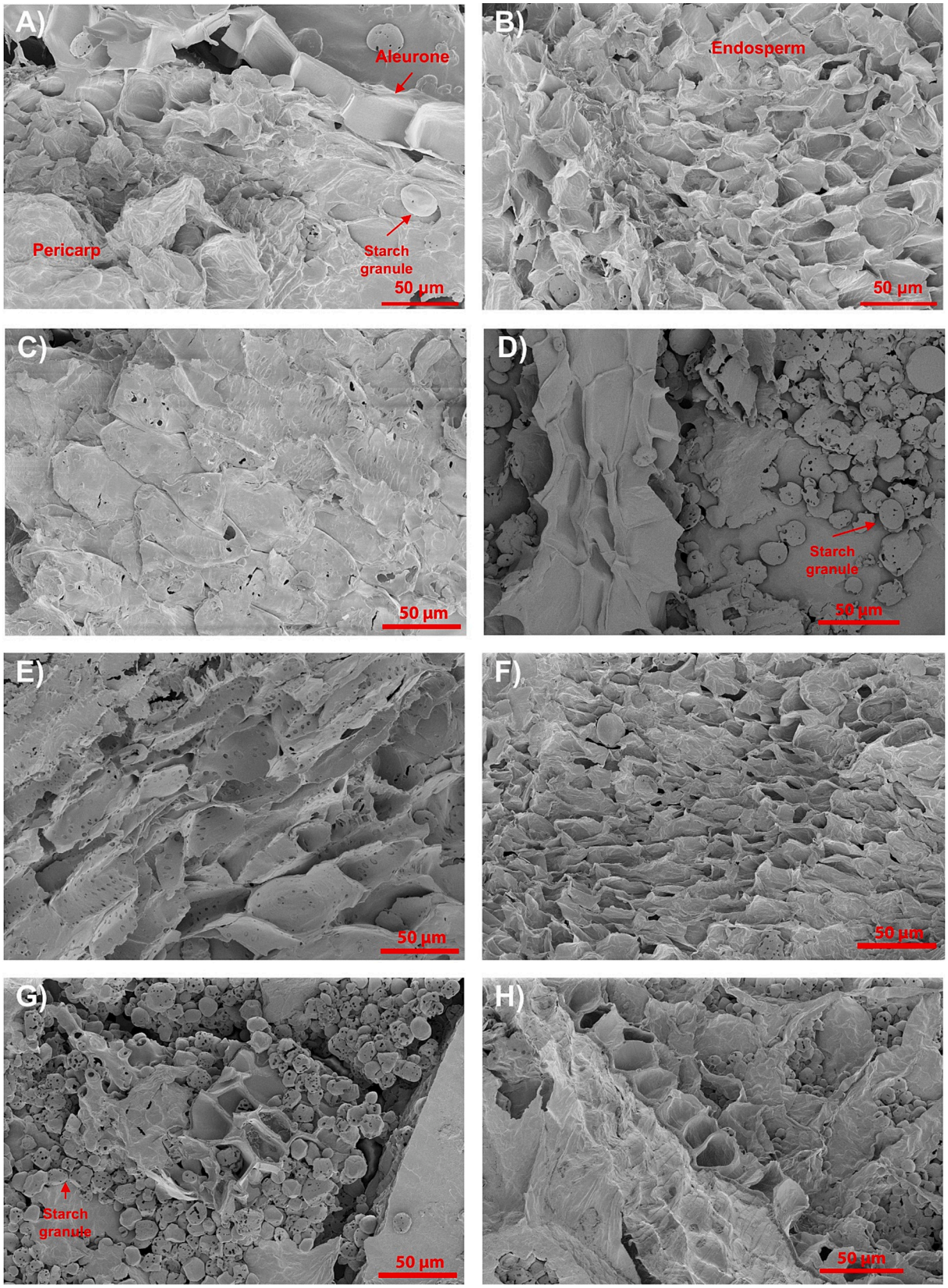

Fig. 5. Scanning Electron Microscopic images of digesta generated at the end (480 min) of *in vitro* digestion of wheat whole grains without (Wheat-Untr; **A**,**B**,**C**) and with HX + EG7 addition (Wheat-HX + EG7; **D**,**E**,**F**) and that of maize grains without (Maize-Untr; **G**) and with HX + EG7 addition (Maize-HX + EG7; **H**).

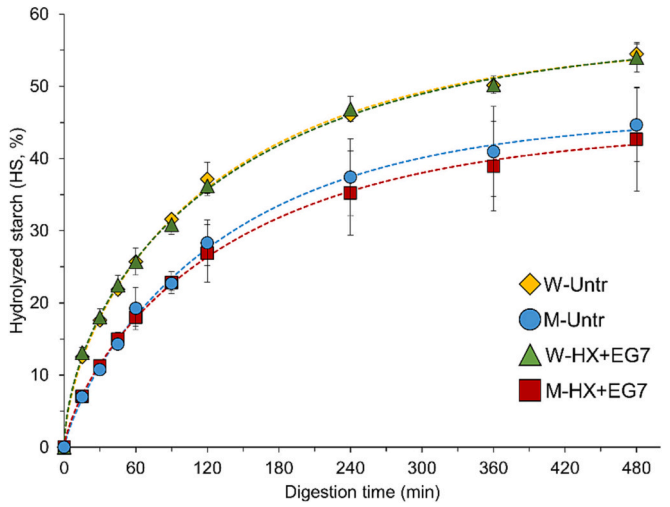

Fig. 6. Starch hydrolysis (% of total starch) during *in vitro* digestion under small intestine conditions of wheat whole grain without (W-Untr: ◆) or with HX and EG7 addition (W-HX + EG7: ▲), and maize whole grain without (M-Unt: ●) or with HX and EG7 addition (M-HX + EG7: ■). Theoretical models (dotted lines) were fitted to the data. Error bars indicate standard deviation ($n = 3$).

Table 2
Kinetic parameters of *in vitro* starch digestion. The significance of treatment on kinetic parameters was assessed by one-way ANOVA, followed by Tukey's HSD test. Values in the same row not sharing common superscript letter differ significantly ($P < 0.05$).

Parameter	W-Untr	W-HX + EG7	M-Untr	M-HX + EG7	*P* value	SEM
HS_{max} (% total starch)	56.3^{ab}	57.0^{a}	45.8^{b}	44.6^{b}	0.020	3.88
k (min^{-1})	5.3 * 10^{-3}	4.8 * 10^{-3}	6.2 * 10^{-3}	5.6 * 10^{-3}	0.371	0.75 * 10^{-3}
n (dimensionless)	0.6	0.6	0.8	0.7	0.058	0.08
RMSE	0.6	0.5	0.7	0.4	–	–

SEM: standard error of the mean for $n = 3$. RMSE: root mean square error.

Vangsøe et al., 2021). Still, oligosaccharide release was also observed for M-AIS (Fig. 4C). The differences observed between substrates could be attributed, for example, to the pronounced recalcitrance to *endo*-xylanases of maize GAX compared to wheat AX due to the more heavily substituted GAX structure (Bach Knudsen, 2014; Dodd & Cann, 2009). Moreover, covalent or non-covalent interactions between hemicellulose, cellulose and lignin might have hindered enzymatic action in all cases (Bach Knudsen, 2014; Dodd & Cann, 2009; Yue et al., 2022). *Endo*-glucanase was successful in degrading NSP from M-AIS showcasing its potential for its use in maize diets (Cowieson et al., 2010; Meng & Slominski, 2005). Insoluble NSP deriving from cereal cell walls have been shown to be excreted unfermented in broilers (Kim et al., 2022). Therefore, the *in situ* conversion of insoluble NSP to oligosaccharides with prebiotic potential is considered beneficial for intestinal health (Bedford, 2018; Broekaert et al., 2011). In particular, the release of DP 2–4 XOS and mono- and di-substituted AXOS as well as gluco-oligosaccharides from W-AIS (Fig. 2E) is considered desirable, as these oligomers are known to be readily fermented by gut microbiota (Broekaert et al., 2011; Zeng et al., 2023). In addition, the formation of feruloylated AXOS could be considered beneficial due to their prebiotic and antioxidant properties (Broekaert et al., 2011). It is noteworthy that the extent and profile of AXOS release *in vitro* was in accordance with AXOS patterns obtained *in vivo* for broilers (Kouzounis et al., 2022). In contrast, the proportion of enzymatically released NSP was relatively low for M-AIS. Consequently, improving NSP fermentability by dietary enzymes is expected to be more promising in wheat than in maize diets. Overall, it is shown that the present *in vitro* model can be applied to assess the potential of feed enzymes to degrade cereal NSP and release oligosaccharides with prebiotic potential.

Apart from improving NSP fermentation, NSPases have been envisaged to offset nutrient encapsulation by the cell wall matrix, thus promoting digestion (Bedford, 2018; Zaefarian et al., 2015). Nevertheless, our study demonstrated that in spite of degrading insoluble NSP, NSPases did not impact *in vitro* starch digestion kinetics. This could be partly explained by the fact that *endo*-xylanase mainly degraded soluble AX in the gizzard phase, whereas insoluble cell wall hydrolysis by NSPases proceeded in parallel with nutrient digestion under *in vitro* small intestine conditions. In contrast, an increase in starch digestion rate was observed when wheat flour was extensively pretreated with *endo*-xylanase, prior to *in vitro* digestion (Korompokis et al., 2019). Aiming for an earlier onset of cell wall hydrolysis by feed NSPases might be desirable for improving nutrient digestion *in vivo*.

NSPase addition has been previously shown to increase *in vitro* starch and protein release from cereal grains and other feedstock alike (Lafond et al., 2015; Meng et al., 2005; Tervilä-Wilo et al., 1996). These different outcomes, compared to our study, could be explained by the fact that nutrient encapsulation is strongly related to the degree of grain intactness (Bhattarai et al., 2018; Grundy et al., 2022). For example, grains were previously milled using 1–3 mm screens (Grundy et al., 2022; Lafond et al., 2015; Tervilä-Wilo et al., 1996), whereas they were presently milled using a 0.5 mm screen, prior to *in vitro* digestion. Whole grains were more extensively milled in the present study in order to better represent the size of feed particles entering the broiler jejunum after grinding in the gizzard (Amerah et al., 2007). As a consequence of milling, our feedstock exhibited low grain intactness (Fig. 5), which was expected to be lower than in previous studies. Most likely, low grain intactness reduced the encapsulating effect of cell wall NSP as shown by the limited lag phase during starch hydrolysis (Fig. 6; Table 2).

Although nutrient de-encapsulation has been previously demonstrated *in vitro*, its occurrence *in vivo* has been questioned (Bedford, 2018; Khadem et al., 2016). The present findings seem to suggest that the lack of improvement in *in vitro* starch digestion kinetics, under relatively optimal conditions, is expected to translate to limited nutrient de-encapsulation *in vivo*. Yet, comparison of our findings with previous studies indicates that several factors, including digestion model, digestive enzyme type and dose, feed enzyme type and dose and grain intactness, need to be considered in such a study. Consequently, follow-up *in vitro* research is warranted to further explore the full potential of feed enzymes to de-encapsulate starch or other nutrients from feed matrices with various degrees of intactness.

4. Conclusions

The present study demonstrates that *endo*-xylanase supplementation in wheat-based diets is essential for offsetting the anti-nutritive effect of soluble, polymeric AX and for releasing oligosaccharides with prebiotic potential. In addition, the combined degradation of AX and glucan(s) from wheat by *endo*-xylanase and *endo*-glucanase, respectively, generated a diverse oligosaccharide profile *in vitro*, that may be beneficial for hindgut fermentation. Furthermore, the present study highlights the ability of *endo*-glucanase to degrade maize cell wall NSP. In this case, the relatively low amounts of oligomers released should be considered in the context of hindgut fermentation. Comparison of our findings with previous studies suggests that grain intactness and the extent of NSP hydrolysis in the upper GIT greatly determine the ability of NSPases to offset nutrient encapsulation. The *in vitro* model introduced in this study aimed at investigating NSPase action during feed digestion in the poultry GIT. Although this model may not be yet fully representative of *in vivo* digestion in poultry, it can be used to evaluate NSPase action on soluble and insoluble NSP and starch digestion kinetics for various feedstock. Finally, the current findings concur in the usefulness of *in vitro* approaches for monitoring NSPase action on NSP from feedstock.

CRediT authorship contribution statement

Dimitrios Kouzounis: Conceptualization, Formal analysis, Investigation, Methodology, Visualization, Writing – original draft. **Khoa A. Nguyen:** Formal analysis, Writing – review & editing. **Cynthia E. Klostermann:** Formal analysis, Writing – review & editing. **Natalia Soares:** Resources, Writing – review & editing. **Mirjam A. Kabel:** Conceptualization, Supervision, Writing – review & editing. **Henk A. Schols:** Conceptualization, Supervision, Writing – review & editing.

Declaration of competing interest

Natalia Soares is employed by the funder. All other authors declare that they have no competing interest.

Data availability

Data will be made available on request.

Acknowledgements

The project has been funded by Huvepharma NV.

Appendix A. Supplementary data

Supplementary data to this article can be found online at https://doi.org/10.1016/j.carbpol.2024.121861.

References

Amerah, A. M., Lentle, R. G., & Ravindran, V. (2007). Influence of feed form on gizzard morphology and particle size spectra of duodenal digesta in broiler chickens. *The Journal of Poultry Science, 44*(2), 175–181. https://doi.org/10.2141/jpsa.44.175

Appeldoorn, M. M., Kabel, M. A., van Eylen, D., Gruppen, H., & Schols, H. A. (2010). Characterization of oligomeric xylan structures from corn fiber resistant to pretreatment and simultaneous saccharification and fermentation. *Journal of Agricultural and Food Chemistry, 58*(21), 11294–11301. https://doi.org/10.1021/jf102849x

Bach Knudsen, K. E. (1997). Carbohydrate and lignin contents of plant materials used in animal feeding. *Animal Feed Science and Technology, 67*(4), 319–338. https://doi.org/10.1016/S0377-8401(97)00009-6

Bach Knudsen, K. E. (2014). Fiber and nonstarch polysaccharide content and variation in common crops used in broiler diets. *Poultry Science, 93*(9), 2380–2393. https://doi.org/10.3382/ps.2014-03902

Barron, C., Surget, A., & Rouau, X. (2007). Relative amounts of tissues in mature wheat (*Triticum aestivum* L.) grain and their carbohydrate and phenolic acid composition. *Journal of Cereal Science, 45*(1), 88–96. https://doi.org/10.1016/j.jcs.2006.07.004

Bautil, A., Buyse, J., Goos, P., Bedford, M. R., & Courtin, C. M. (2021). Feed endoxylanase type and dose affect arabinoxylan hydrolysis and fermentation in ageing broilers. *Animal Nutrition, 7*(3), 787–800. https://doi.org/10.1016/j.aninu.2020.11.015

Becker, D., Braet, C., Brumer, H., Claeyssens, M., Divne, C., Fagerström, B. R., … Wohlfahrt, G. (2001). Engineering of a glycosidase Family 7 cellobiohydrolase to more alkaline pH optimum: The pH behaviour of *Trichoderma reesei* Cel7A and its E223S/ A224H/L225V/T226A/D262G mutant. *Biochemical Journal, 356*(1), 19–30. https://doi.org/10.1042/bj3560019

Bedford, M. R. (2018). The evolution and application of enzymes in the animal feed industry: The role of data interpretation. *British Poultry Science, 59*(5), 486–493. https://doi.org/10.1080/00071668.2018.1484074

Benamrouche, S., Croônier, D., Debeire, P., & Chabbert, B. (2002). A chemical and histological study on the effect of (1 → 4)-β-endo-xylanase treatment on wheat bran. *Journal of Cereal Science, 36*(2), 253–260. https://doi.org/10.1006/jcrs.2001.0427

Bhattarai, R. R., Dhital, S., Mense, A., Gidley, M. J., & Shi, Y. C. (2018). Intact cellular structure in cereal endosperm limits starch digestion *in vitro*. *Food Hydrocolloids, 81*, 139–148. https://doi.org/10.1016/j.foodhyd.2018.02.027

Broekaert, W. F., Courtin, C. M., Verbeke, K., van de Wiele, T., Verstraete, W., & Delcour, J. A. (2011). Prebiotic and other health-related effects of cereal-derived arabinoxylans, arabinoxylan-oligosaccharides, and xylooligosaccharides. *Critical Reviews in Food Science and Nutrition, 51*(2), 178–194. https://doi.org/10.1080/10408390903044768

Brownlee, I. A., Gill, S., Wilcox, M. D., Pearson, J. P., & Chater, P. I. (2018). Starch digestion in the upper gastrointestinal tract of humans. *Starch - Stärke, 70*(9–10), Article 1700111. https://doi.org/10.1002/star.201700111

Bustos, M. C., Vignola, M. B., Pérez, G. T., & León, A. E. (2017). In vitro digestion kinetics and bioaccessibility of starch in cereal food products. *Journal of Cereal Science, 77*, 243–250. https://doi.org/10.1016/j.jcs.2017.08.018

Choct, M., & Annison, G. (1992). Anti-nutritive effect of wheat pentosans in broiler chickens: Roles of viscosity and gut microflora. *British Poultry Science, 33*(4), 821–834. https://doi.org/10.1080/00071669208417524

Cowieson, A. J., Bedford, M. R., & Ravindran, V. (2010). Interactions between xylanase and glucanase in maize-soy-based diets for broilers. *British Poultry Science, 51*(2), 246–257. https://doi.org/10.1080/00071661003789347

Deshors, M., Guais, O., Neugnot-Roux, V., Cameleyre, X., Fillaudeau, L., & Francois, J. M. (2019). Combined *in situ* physical and *ex-situ* biochemical approaches to investigate in vitro deconstruction of destarched wheat bran by enzymes cocktail used in animal nutrition. *Frontiers in Bioengineering and Biotechnology, 7*. https://doi.org/10.3389/fbioe.2019.00158

Dodd, D., & Cann, I. K. O. (2009). Enzymatic deconstruction of xylan for biofuel production. *GCB Bioenergy, 1*(1), 2–17. https://doi.org/10.1111/j.1757-1707.2009.01004.x

Elkin, R. G. (2002). Nutritional components of feedstuffs: A qualitative chemical appraisal of protein. In J. M. McNab, & K. N. Boorman (Eds.), *Poultry feedstuffs: Supply, composition and nutritive value* (pp. 65–86). CABI Publishing. doi: 9780851994642.

Englyst, H. N., Kingman, S. M., & Cummings, J. H. (1992). Classification and measurement of nutritionally important starch fractions. *European Journal of Clinical Nutrition, 46*(Suppl. 2), S33–S50.

Fincher, G. B., & Stone, B. (2004). Chemistry of nonstarch polysaccharides. In C. Wrigley (Ed.), *Encyclopedia of grain science* (pp. 206–223). Elsevier Academic Press. https://doi.org/10.1016/B0-12-765490-9/00107-5.

Flint, H. J., Scott, K. P., Duncan, S. H., Louis, P., & Forano, E. (2012). Microbial degradation of complex carbohydrates in the gut. *Gut Microbes, 3*(4), 289–306. https://doi.org/10.4161/gmic.19897

Gartaula, G., Dhital, S., Pleming, D., & Gidley, M. J. (2017). Isolation of wheat endosperm cell walls: Effects of non-endosperm flour components on structural analyses. *Journal of Cereal Science, 74*, 165–173. https://doi.org/10.1016/j.jcs.2017.02.004

Gerrits, W. J. J., Bosch, M. W., & van den Borne, J. J. G. C. (2012). Quantifying resistant starch using novel, *in vivo* methodology and the energetic utilization of fermented starch in pigs. *The Journal of Nutrition, 142*(2), 238–244. https://doi.org/10.3945/jn.111.147496

Grundy, M. M. L., Tang, J., van Milgen, J., & Renaudeau, D. (2022). Cell wall of feeds and their impact on protein digestibility: An *in vitro* method applied for pig nutrition. *Animal Feed Science and Technology, 293*. https://doi.org/10.1016/j.anifeedsci.2022.115467

Gruppen, H., Hoffmaann, R. A., Kormelink, F. J. M., Voragen, A. G. J., Kamerling, J. P., & Vliegenthart, J. F. G. (1992). Characterisation by 1H NMR spectroscopy of enzymically derived oligosaccharides from alkali-extractable wheat-flour arabinoxylan. *Carbohydrate Research, 233*, 45–64. https://doi.org/10.1016/S0008-6215(00)90919-4

Hernandez-Hernandez, O., Olano, A., Rastall, R. A., & Moreno, F. J. (2019). *In vitro* digestibility of dietary carbohydrates: Toward a standardized methodology beyond amylolytic and microbial enzymes. *Frontiers in Nutrition, 6*, 1–5. https://doi.org/10.3389/fnut.2019.00061

Kabel, M. A., Carvalheiro, F., Garrote, G., Avgerinos, E., Koukios, E., Parajó, J. C., … Voragen, A. G. J. (2002). Hydrothermally treated xylan rich by-products yield different classes of xylo-oligosaccharides. *Carbohydrate Polymers, 50*(1), 47–56. https://doi.org/10.1016/S0144-8617(02)00045-0

Karlsson, J., Siika-Aho, M., Tenkanen, M., & Tjerneld, F. (2002). Enzymatic properties of the low molecular mass endoglucanases Cel12A (EG III) and Cel45A (EG V) of *Trichoderma reesei*. *Journal of Biotechnology, 99*(1), 63–78. https://doi.org/10.1016/S0168-1656(02)00156-6

Khadem, A., Lourenço, M., Delezie, E., Maertens, L., Goderis, A., Mombaerts, R., … Janssens, G. P. J. (2016). Does release of encapsulated nutrients have an important role in the efficacy of xylanase in broilers? *Poultry Science, 95*(5), 1066–1076. https://doi.org/10.3382/ps/pew002

Kim, E., Morgan, N. K., Moss, A. F., Li, L., Ader, P., & Choct, M. (2022). Characterisation of undigested components throughout the gastrointestinal tract of broiler chickens fed either a wheat- or maize-based diet. *Animal Nutrition, 8*(1), 153–159. https://doi.org/10.1016/j.aninu.2021.09.011

Klostermann, C. E., Endika, M. F., ten Cate, E., Buwalda, P. L., de Vos, P., Bitter, J. H., … Schols, H. A. (2023). Type of intrinsic resistant starch type 3 determines in vitro fermentation by pooled adult faecal inoculum. *Carbohydrate Polymers, 319*. https://doi.org/10.1016/j.carbpol.2023.121187

Korompokis, K., de Brier, N., & Delcour, J. A. (2019). Differences in endosperm cell wall integrity in wheat (*Triticum aestivum* L.) milling fractions impact on the way starch responds to gelatinization and pasting treatments and its subsequent enzymatic in vitro digestibility. *Food & Function, 10*(8), 4674–4684. https://doi.org/10.1039/c9fo00947g

Kouzounis, D., Hageman, J. A., Soares, N., Michiels, J., & Schols, H. A. (2021). Impact of xylanase and glucanase on oligosaccharide formation, carbohydrate fermentation patterns, and nutrient utilization in the gastrointestinal tract of broilers. *Animals, 11*(5), 1285. https://doi.org/10.3390/ani11051285

Kouzounis, D., Jonathan, M. C., Soares, N., Kabel, M. A., & Schols, H. A. (2022). *In vivo* formation of arabinoxylo-oligosaccharides by dietary endo-xylanase alters arabinoxylan utilization in broilers. *Carbohydrate Polymers, 291*, Article 119527. https://doi.org/10.1016/j.carbpol.2022.119527

Lafond, M., Bouza, B., Eyrichine, S., Rouffineau, F., Saulnier, L., Giardina, T., Bonnin, E., & Preynat, A. (2015). *In vitro* gastrointestinal digestion study of two wheat cultivars and evaluation of xylanase supplementation. *Journal of Animal Science and Biotechnology, 6*(1), 11–14. https://doi.org/10.1186/s40104-015-0002-7

Marcotuli, I., Hsieh, Y. S. Y., Lahnstein, J., Yap, K., Burton, R. A., Blanco, A., … Gadaleta, A. (2016). Structural variation and content of arabinoxylans in endosperm and bran of durum wheat (*Triticum turgidum* L.). *Journal of Agricultural and Food Chemistry, 64*(14), 2883–2892. https://doi.org/10.1021/acs.jafc.6b00103

Martens, B. M. J., Gerrits, W. J. J., Bruininx, E. M. A. M., & Schols, H. A. (2018). Amylopectin structure and crystallinity explains variation in digestion kinetics of starches across botanic sources in an *in vitro* pig model. *Journal of Animal Science and Biotechnology, 9*(1), 1–13. https://doi.org/10.1186/s40104-018-0303-8

Matthiesen, C. F., Pettersson, D., Smith, A., Pedersen, N. R., & Storm, A. C. (2021). Exogenous xylanase improves broiler production efficiency by increasing proximal small intestine digestion of crude protein and starch in wheat-based diets of various viscosities. *Animal Feed Science and Technology, 272*, Article 114739. https://doi.org/10.1016/j.anifeedsci.2020.114739

Meng, X., & Slominski, B. A. (2005). Nutritive values of corn, soybean meal, canola meal, and peas for broiler chickens as affected by a multicarbohydrase preparation of cell wall degrading enzymes. *Poultry Science, 84*(8), 1242–1251. https://doi.org/10.1093/ps/84.8.1242

Meng, X., Slominski, B. A., Nyachoti, C. M., Campbell, L. D., & Guenter, W. (2005). Degradation of cell wall polysaccharides by combinations of carbohydrase enzymes and their effect on nutrient utilization and broiler chicken performance. *Poultry Science, 84*(1), 37–47. https://doi.org/10.1093/ps/84.1.37

Morgan, N. K., Keerqin, C., Wallace, A., Wu, S. B., & Choct, M. (2019). Effect of arabinoxylo-oligosaccharides and arabinoxylans on net energy and nutrient utilization in broilers. *Animal Nutrition, 5*(1), 56–62. https://doi.org/10.1016/j.aninu.2018.05.001

Mota de Carvalho, N., Oliveira, D. L., Saleh, M. A. D., Pintado, M. E., & Madureira, A. R. (2021). Importance of gastrointestinal in vitro models for the poultry industry and feed formulations. *Animal Feed Science and Technology, 271*, Article 114730. https://doi.org/10.1016/j.anifeedsci.2020.114730

Muscat, A., de Olde, E. M., de Boer, I. J. M., & Ripoll-Bosch, R. (2020). The battle for biomass: A systematic review of food-feed-fuel competition. *Global Food Security, 25*, Article 100330. https://doi.org/10.1016/j.gfs.2019.100330

Nguyen, K. A., Hennebelle, M., van Duynhoven, J. P. M., Dubbelboer, A., Boerkamp, V. J. P., & Wierenga, P. A. (2024). Mechanistic kinetic modelling of lipid oxidation in vegetable oils to estimate shelf-life. *Food Chemistry, 433*. https://doi.org/10.1016/j.foodchem.2023.137266

Paës, G., Berrin, J. G., & Beaugrand, J. (2012). GH11 xylanases: Structure/function/properties relationships and applications. *Biotechnology Advances, 30*(3), 564–592. https://doi.org/10.1016/j.biotechadv.2011.10.003

Pan, D., & Yu, Z. (2013). Intestinal microbiome of poultry and its interaction with host and diet. *Gut Microbes, 5*(1), 108–119. https://doi.org/10.4161/gmic.26945

Ravn, J. L., Glitsø, V., Pettersson, D., Ducatelle, R., Van Immerseel, F., & Pedersen, N. R. (2018). Combined endo -β-1,4-xylanase and α- l -arabinofuranosidase increases butyrate concentration during broiler cecal fermentation of maize glucurono-arabinoxylan. *Animal Feed Science and Technology, 236*, 159–169. https://doi.org/10.1016/j.anifeedsci.2017.12.012

Regassa, A., & Nyachoti, C. M. (2018). Application of resistant starch in swine and poultry diets with particular reference to gut health and function. *Animal Nutrition, 4*(3), 305–310. https://doi.org/10.1016/j.aninu.2018.04.001

Sanchez, J., Barbut, S., Patterson, R., & Kiarie, E. G. (2021). Impact of fiber on growth, plasma, gastrointestinal and excreta attributes in broiler chickens and turkey poults fed corn- or wheat-based diets with or without multienzyme supplement. *Poultry Science, 100*(8). https://doi.org/10.1016/j.psj.2021.101219

Song, H. T., Gao, Y., Yang, Y. M., Xiao, W. J., Liu, S. H., Xia, W. C., … Jiang, Z. B. (2016). Synergistic effect of cellulase and xylanase during hydrolysis of natural lignocellulosic substrates. *Bioresource Technology, 219*, 710–715. https://doi.org/10.1016/j.biortech.2016.08.035

Svihus, B. (2011). The gizzard: Function, influence of diet structure and effects on nutrient availability. *World's Poultry Science Journal, 67*(2), 207–223. https://doi.org/10.1017/S0043933911000249

Svihus, B., & Itani, K. (2019). Intestinal passage and its relation to digestive processes. *Journal of Applied Poultry Research, 28*(3), 546–555. https://doi.org/10.3382/japr/pfy027

Svihus, B., Choct, M., & Classen, H. L. (2013). Function and nutritional roles of the avian caeca: A review. *World's Poultry Science Journal, 69*(2), 249–264. https://doi.org/10.1017/S0043933913000287

Tervilä-Wilo, A., Parkkonen, T., Morgan, A., Hopeakoski-Nurminen, M., Poutanen, K., Heikkinen, P., & Autio, K. (1996). *In vitro* digestion of wheat microstructure with xylanase and cellulase from Trichoderma reesei. *Journal of Cereal Science, 24*(3), 215–225. https://doi.org/10.1006/jcrs.1996.0054

Tryfona, T., Liang, H. C., Kotake, T., Kaneko, S., Marsh, J., Ichinose, H., … Dupree, P. (2010). Carbohydrate structural analysis of wheat flour arabinogalactan protein. *Carbohydrate Research, 345*(18), 2648–2656. https://doi.org/10.1016/j.carres.2010.09.018

van Boekel, M. A. J. S. (2008). *Kinetic modeling of reactions in foods*. CRC Press. https://doi.org/10.1201/9781420017410

van Gool, M. P., van Muiswinkel, G. C. J., Hinz, S. W. A., Schols, H. A., Sinitsyn, A. P., & Gruppen, H. (2013). Two novel GH11 endo-xylanases from *Myceliophthora thermophila* C1 act differently toward soluble and insoluble xylans. *Enzyme and Microbial Technology, 53*(1), 25–32. https://doi.org/10.1016/j.enzmictec.2013.03.019

van Kempen, T. A. T. G., Pujol, S., Tibble, S., & Balfagon, A. (2007). *In vitro* characterization of starch digestion and its implications for pigs. In J. Wiseman, M. A. Varley, S. McOrist, & B. Kemp (Eds.), *Paradigms in pig science* (pp. 515–525). Nottingham University Press.

van Kempen, T. A. T. G., Regmi, P. R., Matte, J. J., & Zijlstra, R. T. (2010). *In vitro* starch digestion kinetics, corrected for estimated gastric emptying, predict portal glucose appearance in pigs. *Journal of Nutrition, 140*(7), 1227–1233. https://doi.org/10.3945/jn.109.120584

Vangsøe, C. T., Bonnin, E., Joseph-Aime, M., Saulnier, L., Neugnot-Roux, V., & Bach Knudsen, K. E. (2021). Improving the digestibility of cereal fractions of wheat, maize, and rice by a carbohydrase complex rich in xylanases and arabinofuranosidases: An *in vitro* digestion study. *Journal of the Science of Food and Agriculture, 101*(5), 1910–1919. https://doi.org/10.1002/jsfa.10806

Vlasenko, E., Schülein, M., Cherry, J., & Xu, F. (2010). Substrate specificity of family 5, 6, 7, 9, 12, and 45 endoglucanases. *Bioresource Technology, 101*(7), 2405–2411. https://doi.org/10.1016/j.biortech.2009.11.057

Wang, J., Cao, H., Bao, C., Liu, Y., Dong, B., Wang, C., … Liu, S. (2021). Effects of xylanase in corn- or wheat-based diets on cecal microbiota of broilers. *Frontiers in Microbiology, 12*. https://doi.org/10.3389/fmicb.2021.757066

Warren, F. J., Zhang, B., Waltzer, G., Gidley, M. J., & Dhital, S. (2015). The interplay of α-amylase and amyloglucosidase activities on the digestion of starch in *in vitro* enzymic systems. *Carbohydrate Polymers, 117*, 185–191. https://doi.org/10.1016/j.carbpol.2014.09.043

Weurding, R. E., Veldman, A., Veen, W. A. G., van der Aar, P. J., & Verstegen, M. W. A. (2001). Starch digestion rate in the small intestine of broiler chickens differs among feedstuffs. *The Journal of Nutrition, 131*(9), 2329–2335. https://doi.org/10.1093/jn/131.9.2329

Yue, Z., Sun, L. L., Sun, S. N., Cao, X. F., Wen, J. L., & Zhu, M. Q. (2022). Structure of corn bran hemicelluloses isolated with aqueous ethanol solutions and their potential to produce furfural. *Carbohydrate Polymers, 288*. https://doi.org/10.1016/j.carbpol.2022.119420

Zaefarian, F., Abdollahi, M. R., & Ravindran, V. (2015). Starch digestion in broiler chickens fed cereal diets. *Animal Feed Science and Technology, 209*, 16–29. https://doi.org/10.1016/j.anifeedsci.2015.07.020

Zeng, M., van Pijkeren, J., & Pan, X. (2023). Gluco-oligosaccharides as potential prebiotics: Synthesis, purification, structural characterization, and evaluation of prebiotic effect. *Comprehensive Reviews in Food Science and Food Safety, 22*(4), 2611–2651. https://doi.org/10.1111/1541-4337.13156